Available online at www.sciencedirect.com
SCIENCE DIRECT®
Comput. Methods Appl. Mech. Engrg. 192 (2003) 1119–1145
Computer methods in applied mechanics and engineering
www.elsevier.com/locate/cma

A directional damage model

Bibiana Luccioni [a,*], Sergio Oller [b]

[a] CONICET, Instituto de Estructuras Universidad Nacional de Tucumán, Av. Roca 1800, 4000 S.M. de Tucumán, Argentina
[b] Departamento de Resistencia de Materiales y Estructuras en la Ingeniería, Universidad Politécnica de Cataluña, Campus Norte UPC, Gran Capitán S/N, 08034 Barcelona, Spain

Received 21 May 2001; received in revised form 6 September 2002; accepted 19 September 2002

Abstract

A directional damage model for initially isotropic metals and geomaterials is presented in this paper. The model is based on a space transformation using an analogy with the theory of finite strains. As a result, damage is defined by a second order damage tensor. The basic equations of the model are derived from the thermodynamics of irreversible processes. A return-mapping algorithm is developed for the numerical integration of the model. Applications examples presented show that the model is able to reproduce damage-induced anisotropy, with directional stiffness degradation and hardening, under general loading conditions.

Keywords: Damage; Anisotropy; Space transformation; Thermodynamics

1. Introduction

Quasi-brittle materials like concrete present a non-linear stress–strain response mainly due to micro-cracking. In most of the cases these cracks are oriented following the stress history and produce a progressive deterioration of the material elastic stiffness. The initially isotropic material is expected to gradually turn anisotropic.

The problem of damage with oriented directions, normally called anisotropic damage or damaged induced anisotropy, has been studied in the last years due to its application to the representation of the behavior of metals and geomaterials in general.

The predictive ability of damage models strongly depends on the particular choice of the damage variable that is used as a macroscopic approximation to describe the underlying micro-mechanic process [11]. The scalar damage variable firstly defined by Kachanov [12] is not capable of representing the

* Corresponding author. Address: Structures Institute, National University of Tucuman, Juan B. Terán 375, Yerba Buena, Tucumán 4107, Argentina. Tel./fax: +54-381-4364087.
E-mail address: bluccioni@herrera.unt.edu.ar (B. Luccioni).

0045-7825/03/$ - see front matter
doi:10.1016/S0045-7825(02)00577-7

directional damage phenomenon. A great number of models based on damage vectors [13], second order damage tensors [4–8,14,16,21,23,25,27,30–32,34] and fourth order damage tensors [3,14,24,26,29] have been developed to reproduce anisotropic damage in quasi-brittle materials.

Additionally, these models are based on different hypothesis to define the transformation produced by damage [31]: the 'strain equivalence hypothesis' [10,15] and the 'energy equivalence hypothesis' [10,25].

In this paper, the problem is presented from a well-known approach [30–32], based on the formulation of the finite strains theory. Although there is no physical relation between these two phenomena, a mathematical comparison can be made at the level of formulation. In the authors' opinion, the unification of both formulations results in a considerable advantage at the time of implementation in existent computer programs oriented to the study of finite strains.

The bases of the formulation of 'directional damage based in the theory of space transformations' is presented in this paper along with simple application examples that show the capabilities of the model developed.

2. Material nucleation and porosity growth. Physical and mechanical description

Material nucleation and porosity growth is one of the important applications of the directionally damage model here presented. According to Maugin [20], damage is an alteration of the elastic properties due to the fact that, in the course of loading, the effective resisting area diminishes as a result of the generation and expansion of voids and micro-cracks. The damage phenomenon only affects the elastic properties of the material, but normally the plasticity phenomenon can be used as complementary to the damage one to control the irreversibility of the inelastic strain evolution.

In what follows, the phenomenon of nucleation and growth in crystalline metals will be briefly described [2].

There is much evidence on the beginning of failure in bars submitted to tension under room temperature. Normally the failure begins on the natural crystallographic planes, through inter granular fractures, or by growth and/or distortion of voids, that can be simulate using a directionally damage model.

The problem becomes more complicated at high temperatures because there appear effects of thermally activated creep, changes in the metallographic characteristics, diffusion and also re-crystallization of the metal.

For polycrystalline metals the problem can be reduced to three basic types of fracture mechanisms (Fig. 1), as explained by Ashby and Tomkins [1] and Atkins and Mai [2]:

1. Fracture produced by small cracks and voids. This type of phenomenon occurs in the total absence of plasticity and is normally motivated by corrosion and/or abrasion.
2. Fracture effects on small cracks and voids produced by mechanical stresses that exceed the material strength.
3. Separation of crystallographic planes and fractures throughout the grain boundaries, produced by high stress derived from mechanical actions.

Brittle fracture is normally produced along inter-crystallographic planes. The fracture becomes more ductile if distortion mechanisms on the crystal lattice and/or voids or pores are developed.

What is normally understood by a plastic phenomenon is one that produces distortions or permanent deviations on the crystal lattice and/or voids at constant volume. It should be noted that this plastic phenomenon causes neither the formation nor the growth of voids or defects. It must also be assumed that the distortion of voids can lead to a state in which they coalesce, leading to a particular form of ductile

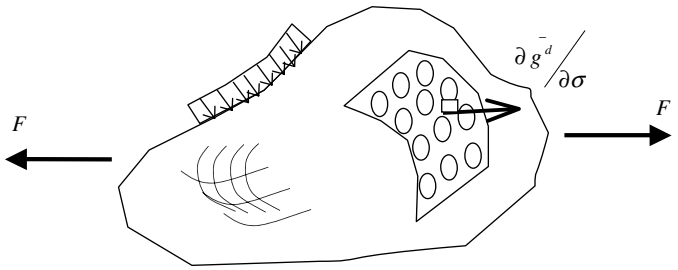

a) Pore and defects nucleation and damage flux orientation

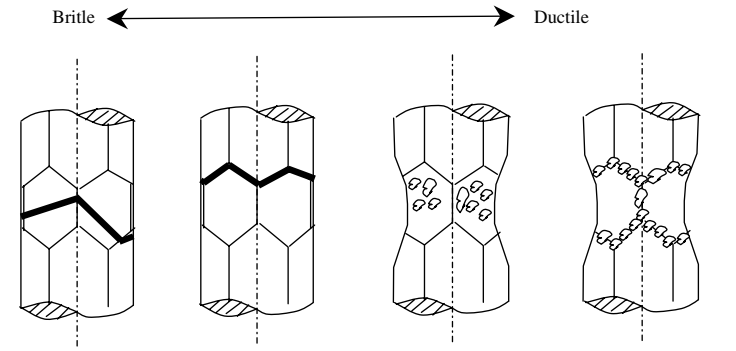

b) Fracture generation.

Fig. 1. Simplest classification of the fracture mechanisms: (a) Pore and defects nucleation and damage flux orientation and (b) fracture generation.

fracture, namely, by shear-fracture bands. A similar kind of fracture occurs when it is produced by an excessive distortion in the crystal lattice of the metal.

In those cases in which there is no creation or nucleation of voids, but the pre-existing ones remain, small in size, under constant volume, it can be assumed that the mechanical behavior can be described by the simplest von Mises plasticity model. This means the voids can be developing permanent distortions only under states of incompressibility.

Complementary to the plasticity phenomenon there appears another, known as damage, that is related to the nucleation and growth of voids and micro-cracks. This phenomenon also leads to the fracture of the material, but in this case by decreasing its effective area. The formulation of this phenomenon is presented in this work, through the directional damage model.

In this paper we propose a broad treatment of the phenomenon of nucleation and growth of defects and voids through a general damage theory that can be coupled with a classical plasticity theory to take into account the distortion of the crystal lattice without volume change too.

The damage theory presented allows taking into account the nucleation and growth of voids and defects and their orientation following a geometric locus whose surface orientation is guided by the normal to a potential damage surface established in the thermodynamic forces space.

3. Damage interpretation

3.1. General formulation

Damage can be mathematically interpreted as a kinematic transformation between two spaces [30–32] (see Fig. 2). For this purpose, a *fictitious non-damaged space*, obtained from the *real damaged space* by removing damage, is defined (see Fig. 2). The material is supposed to behave like the virgin one in the fictitious non-damaged space.

A relation that allows transforming a variable from the fictitious undamaged space to the real damaged space is accepted to exist between the spaces defined. This relation is based on a geometrical change due to damage and can be expressed as a stress and strain space transformation, like a *pull-back* of the second order stress and strain tensors from the undamaged configuration to the damaged one. That is

$$\sigma_{ij} = m_{ik} m^{T}_{jl} \bar{\sigma}_{kl} = M_{ijkl} \bar{\sigma}_{kl}, \tag{1}$$

$$\varepsilon_{ij} = m^{-T}_{ik} m^{-1}_{jl} \bar{\varepsilon}_{kl} = M^{-1}_{ijkl} \bar{\varepsilon}_{kl}, \tag{2}$$

where $\bar{\sigma}_{ij}$, $\bar{\varepsilon}_{ij}$ and σ_{ij}, ε_{ij} are the stresses and strains variables in the undamaged and real spaces, and m_{ij} is a second order transformation tensor like the 'deformation gradient tensor' used in large strains theory. In Eq. (2) it may be observed that the transformation of the strain field results from the concept of conjugate of the stress field through the material constitutive law.

The inverse transformation can be expressed as follows:

$$\bar{\sigma}_{ij} = m^{-1}_{ki} m^{-T}_{lj} \sigma_{kl} = m^{-T}_{ik} m^{-1}_{jl} \sigma_{kl} = M^{-1}_{ijkl} \sigma_{kl}, \tag{3}$$

$$\bar{\varepsilon}_{ij} = m^{T}_{ki} m_{lj} \varepsilon_{kl} = m_{ik} m^{T}_{jl} \varepsilon_{kl} = M_{ijkl} \varepsilon_{kl}. \tag{4}$$

An isotropic constitutive equation correspondent to the virgin material is valid in the fictitious non-damaged space,

$$\bar{\sigma}_{ij} = \overline{C}_{ijkl} \bar{\varepsilon}_{kl}. \tag{5}$$

The constitutive equation in the real space is obtained by replacing Eqs. (4) and (5) in Eq. (1),

$$\begin{aligned} \sigma_{ij} &= M_{ijkl} \bar{\sigma}_{kl} = M_{ijkl} \overline{C}_{klrs} \bar{\varepsilon}_{rs}, \\ \sigma_{ij} &= M_{ijkl} \overline{C}_{klrs} M_{rstu} \varepsilon_{tu}, \\ \sigma_{ij} &= C_{ijtu} \varepsilon_{tu}, \end{aligned} \tag{6}$$

where the secant constitutive tensor C_{ijrs} in the damaged space is expressed as a space transformation like a *pull-back* of the fourth order constitutive tensor from the undamaged configuration to the damaged one. It can be written as

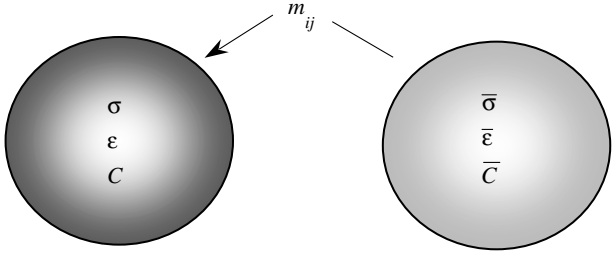

Fig. 2. Correspondence between 'fictitious non-damaged space' and 'real damaged space'.

$$C_{ijrs} = M_{ijkl}\overline{C}_{klmn}M_{mnrs} = m_{ik}m^T_{jl}\overline{C}_{klmn}m_{mr}m^T_{ns}. \tag{7}$$

If the tensor m_{ij} is symmetric, the secant constitutive tensor C_{ijrs} results symmetric but generally non-isotropic.

The strain energy can be written in both damaged and undamaged spaces as

$$W = \tfrac{1}{2}\sigma_{ij}\varepsilon_{ij} = \tfrac{1}{2}M_{ijkl}\bar{\sigma}_{kl}M^{-1}_{ijrs}\bar{\varepsilon}_{rs} = \tfrac{1}{2}I_{klrs}\bar{\sigma}_{kl}\bar{\varepsilon}_{rs} = \tfrac{1}{2}\bar{\sigma}_{kl}\bar{\varepsilon}_{kl} = \overline{W}. \tag{8}$$

From where it is clear, that energy is an invariant respect to space changes, as expected.

In the same way as the 'deformation gradient tensor', the 'second order damage tensor' $\mathbf{m} = m_{ij} = (\partial x_i/\partial \bar{x}_j)$ is a tensor that relates both spaces previously defined. As in the case of directional damage the coordinates transformation defined has not a direct physical interpretation, it is convenient to obtain the tensor $\mathbf{m}$ from other concept. Damage can be conceptually interpreted as a reduction of effective area [12,26]. Thus, the transformation tensor $\mathbf{m}$ can be obtained from the kinematics relation between elemental areas corresponding to both spaces defined [19],

$$\frac{\partial A_i}{\partial \overline{A}_j} = m^{-1}_{ij}|m|, \tag{9}$$

where dA_i is the projection of the elemental effective damaged area dA, over a normal plane to axe x_i and $d\overline{A}_i$ is the projection of the elemental effective undamaged area, $d\overline{A}$, over a normal plane to axe $\bar{x}_i$, see Figs. 3 and 4.

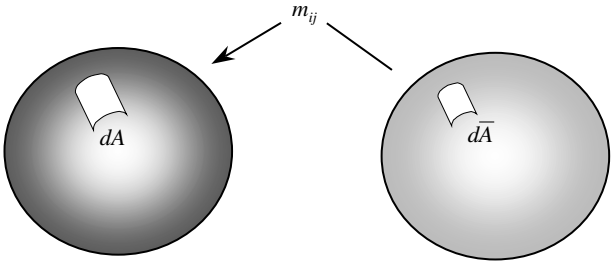

Fig. 3. Correspondence between effective areas.

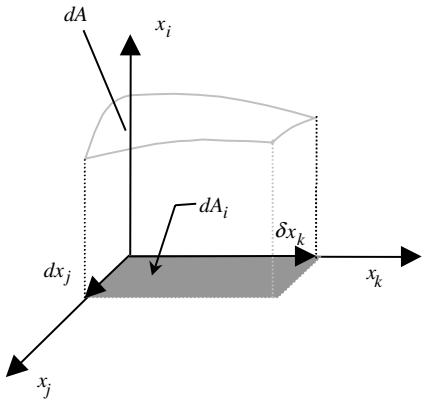

Fig. 4. Elemental effective area.

Evaluating the determinant of expression (9),

$$|m| = \left| \frac{\partial A_r}{\partial \overline{A}_s} \right|^{1/2} \tag{10}$$

and from this equation, the 'second order damage tensor', or 'space transformation tensor' is obtained as a relation between the projections of effective elemental areas,

$$m_{ij} = \left| \frac{\partial A_r}{\partial \overline{A}_s} \right|^{1/2} \left(\frac{\partial A_i}{\partial \overline{A}_j} \right)^{-1}. \tag{11}$$

3.2. Particularization of the formulation to scalar damage case

To illustrate the physical concept that introduces the definition of Eq. (11), the formulation presented is particularized to the case of isotropic scalar damage in this section. For this particular case, the relation between areas can be expressed as

$$\frac{\partial A_i}{\partial \overline{A}_j} = \delta_{ij}(1-d), \tag{12}$$

where δ_{ij} is the delta of Kronecker and d is the scalar damage variable. It must be emphasized that Eq. (12) expresses a relation between effective areas. In that sense, it is coincident with Kachanov's [12] interpretation of damage as a reduction of effective area due to damage.

Replacing the areas relation (12) in Eq. (11), the following expressions for the second order transformation tensor m_{ij} and the fourth order transformation M_{ijkl} are obtained:

$$m_{ij} = (1-d)^{3/2}(1-d)^{-1}\delta_{ij} = (1-d)^{1/2}\delta_{ij}, \tag{13}$$

$$M_{ijkl} = m_{ik}m_{jl}^{T} = (1-d)\delta_{ik}\delta_{jl} = (1-d)I_{ijkl} \tag{14}$$

and replacing in relations (6) the following secant constitutive law can be written:

$$\sigma_{ij} = (1-d)\bar{\sigma}_{ij}, \tag{15}$$

$$\sigma_{ij} = (1-d)\overline{C}_{ijkl}\bar{\varepsilon}_{kl} = (1-d)^2\overline{C}_{ijkl}\varepsilon_{kl} = C_{ijkl}\varepsilon_{kl}, \tag{16}$$

where $C_{ijkl} = (1-d)^2\overline{C}_{ijkl}$ is, in this case, the secant damaged constitutive tensor.

Although Eq. (15) is identical to that corresponding to Kachanov's [12] scalar damage theory, it does not occur the same with Eq. (16) and the secant constitutive tensor. This is due to the fact that Kachanov's theory is based on the assumption of strain equivalence and not in the hypothesis of energy equivalence as the formulation presented here.

3.3. Extension to the case of directional damage

Taking into account that dA_i represents the projection of the elemental effective area against a normal plane to axe x_i defined as [19]

$$dA_i = e_{ijk}dx_j\delta x_k, \tag{17}$$

where e_{ijk} is the permutation symbol, dx_j and δx_k are the edges of the parallelogram with area dA_i (see Fig. 4).

Eq. (12) can be extended to the case of directional damage in the following way:

$$\frac{\partial \widehat{A}_i}{\partial \widehat{\widehat{A}}_j} = [(1-d_1)(1-d_2)(1-d_3)]^{1/2}[(\delta_{ij} - \delta_{ik}\delta_{jk}d_k)^{1/2}]^{-1}. \tag{18}$$

Expanding this expression, the following components can be obtained:

$$\begin{aligned} &\frac{\partial \widehat{A}_1}{\partial \widehat{\widehat{A}}_1} = [(1-d_2)(1-d_3)]^{1/2}, \qquad \frac{\partial \widehat{A}_2}{\partial \widehat{\widehat{A}}_2} = [(1-d_1)(1-d_3)]^{1/2}, \\ &\frac{\partial \widehat{A}_3}{\partial \widehat{\widehat{A}}_3} = [(1-d_1)(1-d_2)]^{1/2}, \qquad \frac{\partial \widehat{A}_1}{\partial \widehat{\widehat{A}}_2} = \frac{\partial \widehat{A}_2}{\partial \widehat{\widehat{A}}_1} = \frac{\partial \widehat{A}_1}{\partial \widehat{\widehat{A}}_3} = \frac{\partial \widehat{A}_3}{\partial \widehat{\widehat{A}}_1} = \frac{\partial \widehat{A}_2}{\partial \widehat{\widehat{A}}_3} = \frac{\partial \widehat{A}_3}{\partial \widehat{\widehat{A}}_2} = 0, \end{aligned} \tag{19}$$

where the upper symbol $\hat{}$ is used to indicate that principal damage directions are taken as reference and d_k are the principal values of the damage tensor d_{ij}, which referred to the principal directions of damage, results diagonal,

$$\hat{d}_{ij} = \delta_{ik}\delta_{jk}d_k, \qquad \hat{m}_{ij} = \delta_{ij} - \hat{d}_{ij}. \tag{20}$$

Eqs. (19) show "in-plane" damage reduction of the area, or 'in-plane' effective area, represented by its index coincident with the outside normal vector to this elementary surface.

Replacing expressions (19) in Eq. (11) the definition of the second order damage tensor, or space transformation tensor, for this case is obtained,

$$\left| \frac{\partial \widehat{A}_i}{\partial \widehat{\widehat{A}}_j} \right| = (1-d_1)(1-d_2)(1-d_3), \tag{21}$$

$$\hat{m}_{ij} = \left| \frac{\partial \widehat{A}_r}{\partial \widehat{\widehat{A}}_s} \right|^{1/2} \left(\frac{\partial \widehat{A}_i}{\partial \widehat{\widehat{A}}_j} \right)^{-1} = (\delta_{ij} - \delta_{ik}\delta_{jk}d_k)^{1/2}, \tag{22}$$

$$m_{ij} = a_{ik}a_{jl}\hat{m}_{kl} = a_{ik}a_{jl}(\delta_{kl} - \delta_{km}\delta_{lm}d_m)^{1/2}, \tag{23}$$

where $a_{ij} = \cos(x_i, \hat{x}_j)$.

From Eq. (23) it is evident that tensor m_{ij} results symmetric and, thus, the symmetry of the secant constitutive elastic tensor is assured, as indicated previously.

The fourth order damage tensor can be expressed as follows:

$$\widehat{M}_{ijkl} = \hat{m}_{ik}\hat{m}^T_{jl} = (\delta_{ik} - \delta_{im}\delta_{km}d_m)^{1/2}(\delta_{jl} - \delta_{jn}\delta_{ln}d_n)^{1/2}, \tag{24}$$

$$M_{ijkl} = a_{im}a_{jn}a_{kr}a_{ls}\widehat{M}_{mnrs} = a_{im}a_{kr}a_{jn}a_{ls}\hat{m}_{mr}\hat{m}^T_{ns}. \tag{25}$$

4. Thermodynamic basis and definition of the directional damage model

A dual description of the thermodynamic foundations of the model is presented in this section. A first form based in the 'primary field', where the free variable of the problem is the strain, is described and then an alternative based on the 'complementary field', where the free variable is the stress, is presented too. This last definition is introduced in order to define the damage flow rule in which the preferential directions of damage are contained. The thermodynamic variables are chosen taking into account the interpretation of damage presented in previous section.

4.1. Thermodynamics basis in the primary field

4.1.1. Free energy and variables of the problem

The specific free energy is defined as follows:

$$\Psi(\varepsilon_{ij},\chi_i)=\tfrac{1}{2}\varepsilon_{ij}C_{ijkl}(m_{rs})\varepsilon_{kl}+\tfrac{1}{2}\alpha_i K_{ij}(m_{rs})\alpha_j, \tag{26}$$

where ε_{ij} is the strain tensor and constitutes the free variable of the problem. $\chi_i=\{m_{ij},\alpha_i\}$ represents the set of internal variables needed to the behavior control of a solid undergoing directional damage. These internal variables are composed of the second order damage tensor m_{ij} and the internal hardening variable α_j. The hardening tensor $K_{ij}(m_{rs})$ and the damaged constitutive tensor $C_{ijkl}(m_{rs})$ depends on the evolution of the internal damage variable m_{ij}.

4.1.2. Mechanical dissipation

According to the second thermodynamics law [19] and taking into account the expression proposed for the free energy, the mechanical dissipation per unit of volume results,

$$\Xi_m=-\dot{\Psi}+\sigma_{ij}\dot{\varepsilon}_{ij}=\left(\sigma_{ij}-\frac{\partial\Psi}{\partial\varepsilon_{ij}}\right)\dot{\varepsilon}_{ij}-\frac{\partial\Psi}{\partial\chi_i}\dot{\chi}_i\geqslant 0. \tag{27}$$

After stating the Coleman's conditions sufficient to assure a non-negative dissipation $\Xi_m\geqslant 0$ [18], the constitutive equations for the solid result,

$$\begin{aligned}&\text{Constitutive equation}\quad \sigma_{ij}=\frac{\partial\Psi}{\partial\varepsilon_{ij}},\\ &\text{Conjugate internal variable}\quad Y_i=-\frac{\partial\Psi}{\partial\chi_i},\\ &\text{Primary field dissipation}\quad \Xi_m=Y_i\dot{\chi}_i\geqslant 0.\end{aligned} \tag{28}$$

The conjugate internal variables can be obtained and grouped as follows:

$$\mathbf{Y}=Y_i=\left\{\begin{array}{c}-\dfrac{\partial\Psi}{\partial\mathbf{m}}\\ \hline -\dfrac{\partial\Psi}{\partial\alpha}\end{array}\right\}=\left\{\begin{array}{c}\mathbf{y}^m\\ \hline \mathbf{q}^\alpha\end{array}\right\}=\bar{\chi}, \tag{29}$$

where $\mathbf{y}^m$ is the conjugate internal variable of the internal damage variable $\mathbf{m}$ and $\mathbf{q}^\alpha$ represents the conjugate variables of the internal hardening variables $\boldsymbol{\alpha}$.

The following expression for the conjugate internal variables are obtained from definitions of Eq. (29):

$$\begin{aligned}&\mathbf{y}^m=y^m_{ij}=-\frac{\partial\Psi}{\partial m_{ij}}=-\frac{1}{2}\varepsilon_{kl}\frac{\partial C_{klpq}}{\partial m_{ij}}\varepsilon_{pq}=-\frac{1}{2}\varepsilon_{kl}\frac{\partial(M_{klrs}\overline{C}_{rsmn}M_{mnpq})}{\partial m_{ij}}\varepsilon_{pq}=-\frac{1}{2}\varepsilon_{kl}\frac{\partial(m_{kr}m^t_{ls}\overline{C}_{rsmn}m_{mp}m^t_{nq})}{\partial m_{ij}}\varepsilon_{pq},\\ &y^m_{ij}=-\tfrac{1}{2}[\varepsilon_{il}m^t_{ls}\overline{C}_{jsmn}m_{mp}m^t_{nq}\varepsilon_{pq}+\varepsilon_{kj}m_{kr}\overline{C}_{rimn}m_{mp}m^t_{nq}\varepsilon_{pq}+\varepsilon_{kl}m_{kr}m^t_{ls}\overline{C}_{r\,\mathrm{sin}}m^t_{nq}\varepsilon_{jq}+\varepsilon_{kl}m_{kr}m^t_{ls}\overline{C}_{rsmj}m_{mp}\varepsilon_{pi}],\\ &y^m_{ij}=-\tfrac{1}{2}[\varepsilon_{ir}m^t_{rs}\overline{C}_{jsmn}\bar{\varepsilon}_{mn}+\varepsilon_{rj}m_{rs}\overline{C}_{simn}\bar{\varepsilon}_{mn}+\bar{\varepsilon}^t_{rs}\overline{C}_{rsim}m^t_{mn}\varepsilon_{jn}+\bar{\varepsilon}^t_{rs}\overline{C}_{rsmj}m_{mn}\varepsilon_{ni}],\end{aligned} \tag{30}$$

or written in terms of stress,

$$
\begin{aligned}
y_{ij}^{m} &= -\tfrac{1}{2}[\varepsilon_{ir} m_{rs}^{t} \bar{\sigma}_{js} + \varepsilon_{rj} m_{rs} \bar{\sigma}_{si} + \bar{\sigma}_{im} m_{mn}^{t} \varepsilon_{jn} + \bar{\sigma}_{mj} m_{mn} \varepsilon_{ni}],\\
y_{ij}^{m} &= -\tfrac{1}{2}[\varepsilon_{ir} m_{rs}^{t} m_{jk}^{-t} m_{sl}^{-1} \sigma_{kl} + \varepsilon_{rj} m_{rs} m_{sk}^{-t} m_{il}^{-1} \sigma_{kl} + m_{ik}^{-t} m_{ml}^{-1} \sigma_{kl} m_{mn}^{t} \varepsilon_{jn} + m_{mk}^{-t} m_{jl}^{-1} \sigma_{kl} m_{mn} \varepsilon_{ni}],\\
y_{ij}^{m} &= -\tfrac{1}{2}[\varepsilon_{ir} m_{jk}^{-t} \sigma_{kr} + \varepsilon_{rj} m_{ik}^{-1} \sigma_{rk} + m_{ik}^{-t} \sigma_{kr} \varepsilon_{jr} + m_{jk}^{-1} \sigma_{rk} \varepsilon_{ri}],\\
y_{ij}^{m} &= -\tfrac{1}{2}[C_{irmn}^{-1} \sigma_{mn} m_{jk}^{-t} \sigma_{kr} + C_{rjmn}^{-1} \sigma_{mn} m_{ik}^{-1} \sigma_{rk} + m_{ik}^{-t} \sigma_{kr} C_{jrmn}^{-1} \sigma_{mn} + m_{jk}^{-1} \sigma_{rk} C_{rimn}^{-1} \sigma_{mn}]
\end{aligned}
\tag{31}
$$

and the hardening conjugate variable, results

$$
\mathbf{q}^{\alpha} = q_{i}^{\alpha} = -\frac{\partial \Psi}{\partial \alpha_{i}} = -K_{ij}(m_{rs})\alpha_{j}. \tag{32}
$$

4.2. Thermodynamic basis in the complementary field

4.2.1. Free energy and variables of the problem

The complementary specific free energy can be obtained as a conjugate function of the primary free energy (Eq. (26)), through the Legendre–Fenchel transformation [20,22], that is

$$
\overline{\Psi}(\sigma_{ij}, \bar{\chi}_{i}) = \max_{\varepsilon} \{\sigma_{ij}\varepsilon_{ij} - \Psi(\varepsilon_{ij}, \chi_{i})\} \Rightarrow \overline{\Psi}(\sigma_{ij}, \bar{\chi}_{i}) = \tfrac{1}{2}\sigma_{ij} C_{ijkl}^{-1}(y_{rs}^{m})\sigma_{kl} - \tfrac{1}{2} q_{i}^{\alpha} \overline{K}_{ij}(y_{rs}^{m}) q_{j}^{\alpha}, \tag{33}
$$

where σ_{ij} is the stress tensor and represents the new free variable of the problem. $\bar{\chi}_{i} = \{y_{ij}^{m}, q_{i}^{\alpha}\}$ represents the set of internal variable necessary to the behavior control of the solid undergoing directional damage. These internal variables are composed of the complementary internal damage variable y_{ij}^{m} and the complementary internal hardening variable q_{j}^{α}. The complementary hardening tensor $\overline{K}_{ij}(y_{rs}^{m}) = K_{ij}^{-1}(m_{rs})$ and the damage constitutive tensor $C_{ijkl}(y_{rs}^{m})$ depends on the evolution of the complementary internal damage variable y_{ij}^{m}.

4.2.2. Mechanical dissipation

Following the formulation of the second thermodynamics law [19] and considering the complementary free energy defined in Eq. (33), the mechanical dissipation per unit of volume results,

$$
\overline{\Xi}_{m} = \dot{\overline{\Psi}} - \dot{\sigma}_{ij}\varepsilon_{ij} = \left(\frac{\partial \overline{\Psi}}{\partial \sigma_{ij}} - \varepsilon_{ij}\right)\dot{\sigma}_{ij} + \frac{\partial \overline{\Psi}}{\partial \bar{\chi}_{i}}\dot{\bar{\chi}}_{i} \geqslant 0. \tag{34}
$$

After the application of Colleman's conditions for assuring positive dissipation, the following constitutive equations result [18]:

$$
\begin{aligned}
&\text{Constitutive equation} \quad \varepsilon_{ij} = \frac{\partial \overline{\Psi}}{\partial \sigma_{ij}},\\
&\text{Internal variable} \quad \overline{Y}_{i} = \frac{\partial \overline{\Psi}}{\partial \bar{\chi}_{i}},\\
&\text{Complementary field dissipation} \quad \overline{\Xi}_{m} = \overline{Y}_{i}\dot{\bar{\chi}}_{i} \geqslant 0.
\end{aligned}
\tag{35}
$$

The primary internal variables $\mathbf{m} = m_{ij}$ and the hardening variables $\boldsymbol{\alpha} = \alpha_{i}$ that appear here can be grouped as

$$
\overline{\mathbf{Y}} = \left\{\begin{array}{c} \dfrac{\partial \overline{\Psi}}{\partial \mathbf{y}^{m}} \\ \hline \dfrac{\partial \overline{\Psi}}{\partial \mathbf{q}^{\alpha}} \end{array}\right\} = \left\{\begin{array}{c} \mathbf{m} \\ \hline \alpha \end{array}\right\} = \chi \tag{36}
$$

4.3. Flow damage rule

It is accepted that the primary field dissipation $\Xi_m = Y_i\dot{\chi}_i \geqslant 0$ (Eq. (28)) can be written by means of a convex function of the type $D(\dot{\chi}_i) \geqslant 0$ which only depends on the internal variables $\dot{\chi}_i$ and the thermodynamic state variables at a certain time. A so-called dissipation pseudopotential can then be defined as the following convex function [20]:

$$\varphi(\dot{\chi}_i) = \int_0^t D(t, \dot{\chi}_i)\frac{\mathrm{d}t}{t}. \tag{37}$$

Using this definition, the complementary pseudopotential can be obtained by means of the Legendre–Fenchel transformation [22],

$$\bar{\varphi}(Y_i) = \bar{\varphi}(\bar{\chi}_i) = \max_{\dot{\chi}_i}\{Y_i\dot{\chi}_i - \varphi(\dot{\chi}_i)\}. \tag{38}$$

That is the indicator function of a convex space L in the complementary space and allows defining the evolution of the internal variable $\dot{\chi}_i$, by means of the following normality rule:

$$\begin{aligned} &\dot{\chi}_i = \dot{\lambda}\frac{\partial G(Y_j)}{\partial Y_i} = \dot{\lambda}\frac{\partial G(\bar{\chi}_j)}{\partial \bar{\chi}_i}, \quad \text{with } \dot{\lambda} \geqslant 0 \ \ \forall \mathbf{Y} \in \partial L \quad \text{or } F(\mathbf{Y}) = 0, \\ &\dot{\chi}_i = 0 \quad \forall \mathbf{Y} \in L \quad \text{or } F(\mathbf{Y}) < 0, \end{aligned} \tag{39}$$

where $F = 0$ and $G = 0$ are the equations of convex closed surfaces in the complementary space defined on $Y_i = \bar{\chi}_i$ and $\dot{\lambda}$ is a scalar non-negative factor.

For the particular model presented in this paper, the damage flow rule of Eq. (39), results

$$\dot{\boldsymbol{m}}_{ij} = \begin{cases} \dot{\lambda}\dfrac{\partial G(\mathbf{Y})}{\partial y_{ij}^m} & \text{if } F(\mathbf{Y}) = 0, \\ 0 & \text{if } F(\mathbf{Y}) < 0, \end{cases} \tag{40}$$

$$\dot{\alpha}_i = \begin{cases} \dot{\lambda}\dfrac{\partial G(\mathbf{Y})}{\partial q_i^\alpha} & \text{if } F(\mathbf{Y}) = 0, \\ 0 & \text{if } F(\mathbf{Y}) < 0. \end{cases} \tag{41}$$

Such that F and G represent the damage threshold function and the potential damage function respectively.

4.4. Damage threshold function and damage potential function definition

The following equations are proposed in the present work for the damage threshold function $F(\mathbf{Y})$ and the damage potential function $G(\mathbf{Y})$:

$$\begin{aligned} F &= \sqrt{\frac{1}{2}\tilde{y}_{ij}\tilde{y}_{ij}} - 1 = 0, \\ G &= \sqrt{\frac{1}{2}\tilde{y}_{ij}\tilde{y}_{ij}} - 1 = 0, \end{aligned} \tag{42}$$

where the mapped thermodynamic forces $\tilde{y}_{ij}$ are defined as

$$\tilde{y}_{ij} = \widetilde{A}_{ijkl}\bar{y}_{kl} = \widetilde{A}_{ijkl}\overline{A}_{klrs}y_{rs}^m. \tag{43}$$

$\widetilde{A}_{ijkl}$ is a diagonal transformation tensor which contains information about the directional hardening. For the particular case in which the directions of hardening are uncoupled, a simplified tensor $\widetilde{A}_{ijkl}$, referred to the principal directions of damage, can be written as

$$\widetilde{A}_{ijkl} = B_{ik}C_{jl}, \quad B_{ik} = \frac{E_o}{\sqrt{2}}\delta_{is}\delta_{ks}m_s^5, \quad C_{jl} = \delta_{jr}\delta_{lr}[\sigma(m_r)]^{-2}, \tag{44}$$

where E_o is the elasticity Young modulus of the undamaged material, m_s are the principal values of the m_{ij} damage tensor and $\sigma(m_r)$ the comparison compression strength in "r" direction, obtained from a laboratory uniaxial stress–strain curve.

Tensor $\overline{A}_{ijkl}$ is introduced in order to preserve convexity of the damage threshold surface in both stress space and thermodynamics forces space. Referred to the principal directions of damage, this tensor can be written as follows:

$$\begin{aligned} &\overline{A}_{ijkl} = (n^2-1)\delta_{im}\delta_{jm}\delta_{km}\delta_{lm}r_m + \delta_{im}\delta_{jn}\delta_{km}\delta_{ln}\delta_{mn}, \\ &r_m = \frac{\langle\sigma_m\rangle}{|\sigma_m|} = \begin{cases} 1 & \text{si } \sigma_m > 0, \\ 0 & \text{si } \sigma_m < 0, \end{cases} \quad \text{no sum over '}m\text{'}. \end{aligned} \tag{45}$$

The factor n represents the relation between strength corresponding to damage thresholds in uniaxial compression and uniaxial extension and the σ_m are the values of the normal stresses in the principal damage directions.

4.4.1. Convexity of the damage threshold surface on the thermodynamic forces and the stresses spaces

For $n = 1$, tensor $\overline{A}_{ijkl}$ is the fourth order identity tensor and the damage surface plotted in the σ_S principal stress space looks like that in Fig. 5. The same surface but plotted in the y_S^m principal thermodynamic forces space is shown in Fig. 6. The thermodynamic forces are always negative for any sign combination of stress components. Thus, a circular arc in the third quadrant represents the damage threshold. It is shown that the surface fulfils the thermodynamic hypothesis about the convexity of $F(y_{ij}^m) = 0$.

The tensor $\overline{A}_{ijkl}$, is defined to preserve the convexity of the damage threshold surface in the thermodynamic forces space when $n \neq 1$. The damage threshold surface in the stress space and in the thermodynamic forces space for $n = 5$ are presented in Figs. 7 and 8 respectively.

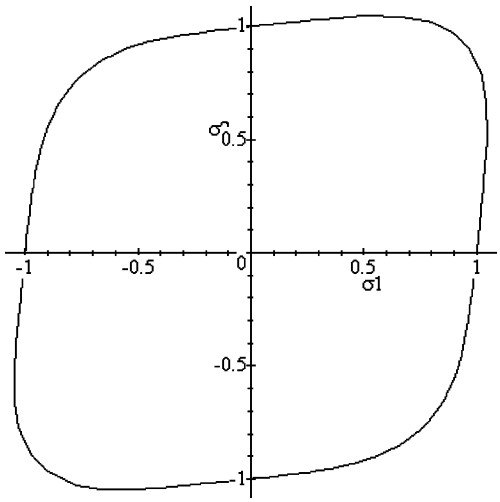

Fig. 5. Damage threshold surface for $n = 1$ in the principal stress plane ($\sigma_{1o} = 1.0$).

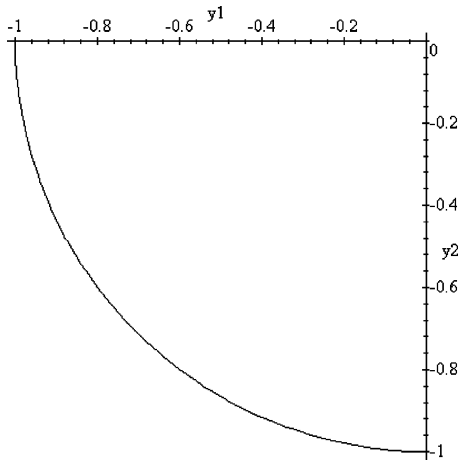

Fig. 6. Damage threshold surface for $n = 1$ in the thermodynamics force space ($y_{1o} = -1$).

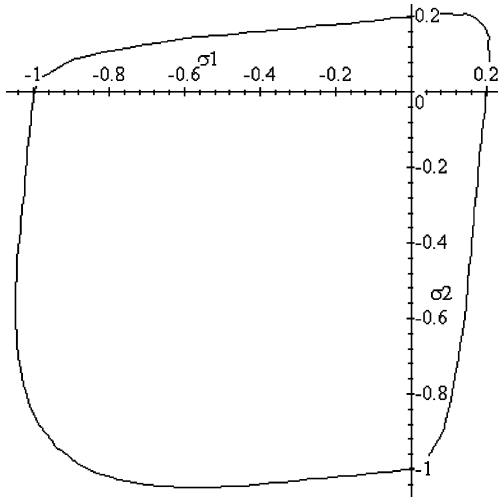

Fig. 7. Damage threshold surface for $n = 5$ in the principal stress plane $\sigma_3 = 0$ ($\sigma_{1o} = 1.0$).

In Fig. 8 the four curves drawn are related with the different sign combinations of the stress components. It is clear that $F(y_{ij}^m) = 0$ results convex for $n \neq 1$.

4.5. Damage evolution law

The damage consistency condition is used to find the consistency factor $\dot{\lambda}$ that defines the internal damage variable evolution (Eqs. (40) and (41)). That is

$$\dot{F}(y_{ij}^m) = 0 \Rightarrow \frac{\partial F}{\partial y_{ij}^m}\left[\frac{\partial y_{ij}^m}{\partial \varepsilon_{kl}}\dot{\varepsilon}_{kl} + \frac{\partial y_{ij}^m}{\partial m_{kl}}\dot{m}_{kl}\right] = 0. \tag{46}$$

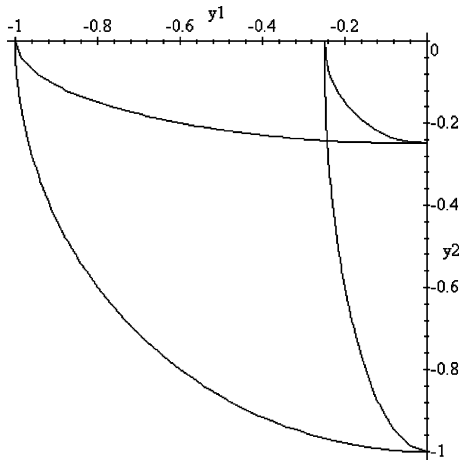

Fig. 8. Damage threshold surface for $n = 5$ in the thermodynamics forces space ($y_{1o} = -1$).

Replacing the damage flow rule (Eq. (40)) in Eq. (46), the consistency factor is obtained,

$$\frac{\partial F}{\partial y_{ij}^m}\left[\frac{\partial y_{ij}^m}{\partial \varepsilon_{kl}}\dot{\varepsilon}_{kl} + \frac{\partial y_{ij}^m}{\partial m_{kl}}\dot{\lambda}\frac{\partial G}{\partial y_{kl}^m}\right] = 0 \Rightarrow \dot{\lambda} = -\frac{\dfrac{\partial F}{\partial y_{ij}^m}\dfrac{\partial y_{ij}^m}{\partial \varepsilon_{kl}}\dot{\varepsilon}_{kl}}{\dfrac{\partial F}{\partial y_{rs}^m}\dfrac{\partial y_{rs}^m}{\partial m_{pq}}\dfrac{\partial G}{\partial y_{pq}^m}} \tag{47}$$

and from here, the tangent elastic tensor can be found. See Appendix A.

4.6. Hardening rule

The definition of damage evolution from uniaxial tests and the shape of the damage threshold during the hardening process are studied in this section. To simplify the interpretation of the results, the case when $n = 1$ is considered.

4.6.1. Hardening function

The function $\sigma(m_r)$ that takes part of the definition of the mapping tensor C_{jl} in Eq. (44) must be known to define damage hardening. This strength function can be obtained from a uniaxial test. Suppose the particular case in which a linear hardening function like those in Fig. 9 is adopted.

Starting from the following equality that represents the uniaxial constitutive damage law and from the uniaxial response curve equations,

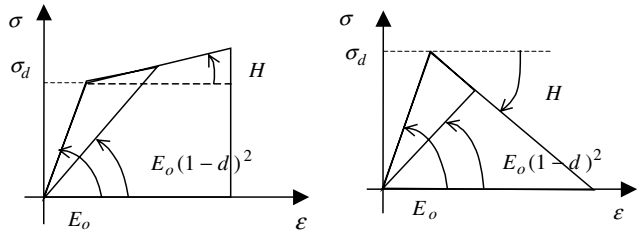

Fig. 9. Uniaxial stress–strain curves with hardening and softening.

$$\sigma(m) = m^4 E_o \varepsilon = \begin{cases} E_o \varepsilon & \text{if } \varepsilon \leqslant \sigma_d / E_o, \\ \sigma_d + H(\varepsilon - \sigma_d / E_o) & \text{if } \varepsilon > \sigma_d / E_o \end{cases} \tag{48}$$

the following results are obtained:

$$\varepsilon = \frac{\sigma(m) - \sigma_d}{H} + \frac{\sigma_d}{E_o} \tag{49}$$

and

$$\sigma(m) = \frac{m^4 E_o \sigma_d}{m^4 E_o - H(1 - m^4)}. \tag{50}$$

The expression of $\sigma(m)$ can be numerically obtained using any other hardening functions $\sigma(\varepsilon)$ different from the linear one described.

4.6.2. Damage threshold surface evolution

The evolution of the damage threshold surface is studied in this section. Particularly the problem of how does loading beyond the damage threshold in one direction affect damage thresholds in orthogonal directions is analyzed.

The initial damage threshold surface (internal) and the final damage threshold surface (external) for a material under uniaxial tension in direction 1 are presented in Fig. 10. The final damage threshold surface corresponds to $m_1 = 0.8$, $m_2 = 1.0$, $m_3 = 1.0$ and $\sigma(m_1) = 1.2\sigma_o$.

It can be verified that hardening in one direction has no influence in the damage threshold in orthogonal directions. This fact is due to the particular definition of $\widetilde{A}_{ijkl}$ in Eq. (44). In fact, a certain degree of coupling is generally present in all materials. This effect can be taken into account replacing definition of tensor C_{ij} in Eq. (44) by the following:

$$C_{ij} = \delta_{ir}\delta_{jr}\{\sigma[(1-\beta)m_r + \beta 1_r \det(m_{kl})]\}^{-2}, \tag{51}$$

where $0 \leqslant \beta \leqslant 1$ defines the degree of coupling and takes the value $\beta = 0$ when there is no coupling, m_r are the damage principal values and 1_r represents a column vector of 1.

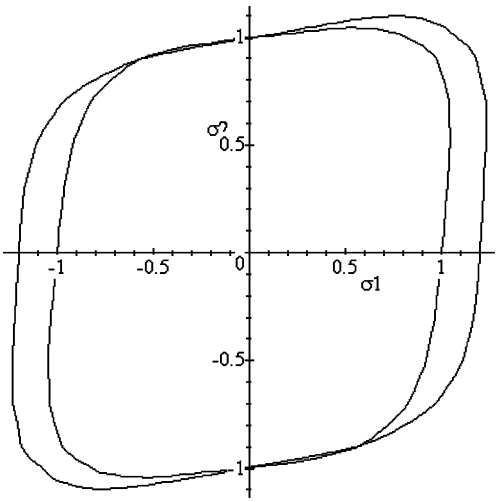

Fig. 10. Initial damage threshold surface (internal) and final (external) damage threshold surface.

5. Numerical implementation

Following the virtual work principle and the first thermodynamic law, the mechanical equilibrium equations under small strain assumption are obtained,

$$\int_V (\dot{\mathbf{u}} \cdot m \cdot \ddot{\mathbf{u}} + \sigma \cdot \nabla^s \dot{\mathbf{u}})\, \mathrm{d}V - \int_V m\mathbf{b}\dot{\mathbf{u}}\, \mathrm{d}V - \oint_S \mathbf{t}\dot{\mathbf{u}}\, \mathrm{d}S = 0, \tag{52}$$

where $\mathbf{u}$, $\dot{\mathbf{u}}$, $\ddot{\mathbf{u}}$ are the field displacement and its temporal derivatives, m is the density, $\mathbf{t}$ are the surface load distributed over the S surface, and $\mathbf{b}$ represents the bulk load in the V volume. Approximating the displacements field $\mathbf{u}(x_i) \cong \mathbf{N}^u(x_i) \cdot \mathbf{U}$ by the standard finite element procedure [35], the following equilibrium equations are obtained:

$$\mathbf{M}_u \cdot \ddot{\mathbf{U}} + \mathbf{f}_u^{\mathrm{int}} - \mathbf{f}_u^{\mathrm{ext}} = \mathbf{0}, \tag{53}$$

where $\mathbf{N}^u(x_i)$ is the displacement shape function, $\mathbf{U}$ is the nodal values of the displacements, $\mathbf{M}_u$ is the mass matrix, $\mathbf{f}_u^{\mathrm{int}} = (f_k)_u^{\mathrm{int}} = \int_V \sigma_{ij} \nabla_i^S N_{jk}^u \, \mathrm{d}V$ is the mechanical internal forces vector, $\mathbf{f}_u^{\mathrm{ext}}$ is the nodal forces vector due to external loads. The solution of these equilibrium equations follows an implicit time integration scheme [35].

The stress tensor contained in the equilibrium equations is obtained by means the 'directional damage constitutive model' whose formulation was detailed in the present paper and its numerical implementation is shown in the algorithm summarized in this section.

A return-mapping algorithm is proposed for the numerical integration of the damage constitutive equations. The damage threshold function is written by means a linearized procedure between two consecutive iterations as shown in next items.

5.1. Integration of directionally damage constitutive equation algorithm

1. Displacement increment for step 'n' is obtained from equilibrium equation written in agreement with the finite element scheme: Δu_i^n.
2. Incremental and updating strains are obtained:

   $$\Delta\varepsilon_{ij}^n = \tfrac{1}{2}(\Delta u_{i,j}^n + \Delta u_{j,i}^n),$$

   $$\varepsilon_{ij}^n = \varepsilon_{ij}^{n-1} + \Delta\varepsilon_{ij}^n.$$
3. Starting with the stress elastic predictor $k = 0$

   $$(m_{ij})_o^n = (m_{ij})^{n-1},$$

   $$(\sigma_{ij})_o^n = (m_{ir})_o^n (m_{js}^t)_o^n \overline{C}_{rstu} (m_{tp})_o^n (m_{uq}^t)_o^n \varepsilon_{pq}^n.$$
4. Damage principal directions are obtained from 'second order damage tensor' m_{ij}:

   $$(a_{ij})_k^n = \cos(x_i, \hat{x}_j).$$
5. Stress, and strain tensors rotated to damage principal directions are computed:

   $$(\hat{\sigma}_{ij})_k^n = (a_{pi}^{-1})_k^n (a_{qj}^{-1})_k^n (\sigma_{pq})_k^n; \quad (\hat{\varepsilon}_{ij})_k^n = (a_{pi}^{-1})_k^n (a_{qj}^{-1})_k^n (\varepsilon_{pq})_k^n.$$
6. Thermodynamics force evaluation (Eqs. (42)–(44)):

   $$(y_{ij}^m)_k^n; \quad (\bar{y}_{ij})_k^n; \quad (\tilde{y}_{ij})_k^n.$$
7. Damage threshold verification:

   If $F[(\tilde{y}_{ij})_k^n] < 0$ elastic behavior. Therefore go to 12.

8. Damage behavior. Starting from iteration $k = k + 1$, reach the damage consistency factor $\Delta\lambda_k$:

$$\text{From} \quad F_k = 0 \Rightarrow \Delta\lambda_k = -\frac{F_{k-1}}{\left(\dfrac{\partial F}{\partial m_{ij}}\right)^n_{k-1}\left(\dfrac{\partial G}{\partial y^m_{ij}}\right)^n_{k-1}}.$$

9. Increment of second order damage tensor:

$$(\Delta\hat{m}_{ij})^n_k = \Delta\lambda_k\left(\frac{\partial G}{\partial y^m_{ij}}\right)^n_{k-1},$$

$$(\Delta m_{ij})^n_k = a_{ir}a_{js}(\Delta\hat{m}_{rs})^n_k.$$

10. Updating of second order damage tensor:

$$(m_{ij})^n_k = (m_{ij})^n_{k-1} + (\Delta m_{ij})^n_k.$$

11. Stress state updating:

$$(\sigma_{ij})^n_k = (m_{ir})^n_k(m^t_{js})^n_k\overline{C}_{rstu}(m_{tp})^n_k(m^t_{uq})^n_k\varepsilon^n_{pq}.$$

12. End of linearized process. Go back to 4.
13. Setting up the stresses, damage and constitutive tensors for next load increment in each integration point:

$$(\sigma_{ij})^n = (\sigma_{ij})^n_k; \quad (m_{ij})^n = (m_{ij})^n_k; \quad (C_{ijpq})^n = (m_{ir})^n_k(m^t_{js})^n_k\overline{C}_{rstu}(m_{tp})^n_k(m^t_{uq})^n_k.$$

14. Computation of the tangent constitutive tensor:

$$(C^T_{ijrs})^n = \left[C_{ijrs} - \frac{\left[\left(\dfrac{\partial G}{\partial y^m_{im}}m^t_{jn} + m_{im}\dfrac{\partial G}{\partial y^m_{nj}}\right)\bar{\sigma}_{mn} + m_{im}m^t_{jn}\overline{C}_{mnpq}\left(\dfrac{\partial G}{\partial y^m_{pk}}m^t_{ql} + m_{pk}\dfrac{\partial G}{\partial y^m_{lq}}\right)\varepsilon_{kl}\right]\dfrac{\partial F}{\partial y^m_{tu}}\dfrac{\partial y^m_{tu}}{\partial\varepsilon_{rs}}}{\dfrac{\partial F}{\partial m_{tu}}\dfrac{\partial G}{\partial y^m_{tu}}}\right]^n.$$

15. End of the constitutive equation integration.

6. Numerical examples

6.1. Numerical test with loading and unloading in two orthogonal directions

The influence of the previous load on the uniaxial strength limit of the orthogonal load direction is an interesting practical problem. In this section the results obtained for an initially isotropic material when it is loaded in a certain direction, then unloaded and loaded in the orthogonal direction as indicated in Fig. 11, are presented.

The proposed material properties are the following:

Initial elastic modulus:	$E_0 = 35\,000$ Mpa
Initial Poisson coefficient:	$\nu = 0.2$
Linear hardening:	$H = 5000$ Mpa
Initial damage threshold in uniaxial compression:	$\sigma_{co} = 30$ Mpa
Strength damage thresholds ratio:	$n = \sigma_{co}/\sigma_{to} = 10$
No directional coupling:	$\beta = 0.$

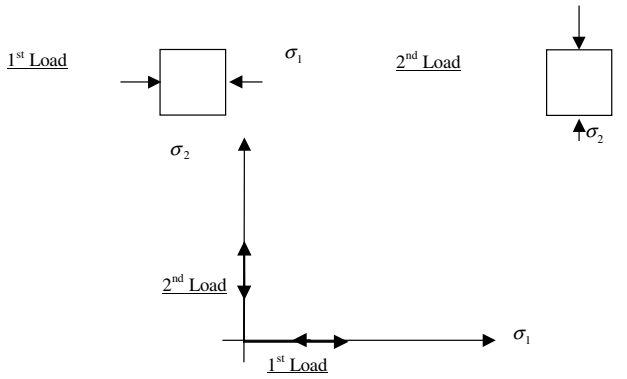

Fig. 11. Loading path in the principal stress space $\sigma_3 = 0$.

For this example, damage principal directions are coincident with principal stress directions and the damage tensor results diagonal,

$$\mathbf{m} = m_{ij} = \begin{bmatrix} \sqrt{1-d_1} & 0 & 0 \\ 0 & \sqrt{1-d_2} & 0 \\ 0 & 0 & 1 \end{bmatrix}.$$

The stress–strain curves obtained for the two loading stages are presented in Fig. 12. It may be observed that the material looses stiffness in the loading direction but not in the orthogonal one.

The damage threshold curves corresponding to the different load stages are represented in the principal stress space in Fig. 13. A directional hardening in the loading direction and not in the orthogonal one is obtained in accordance with the hypothesis of $\beta = 0$.

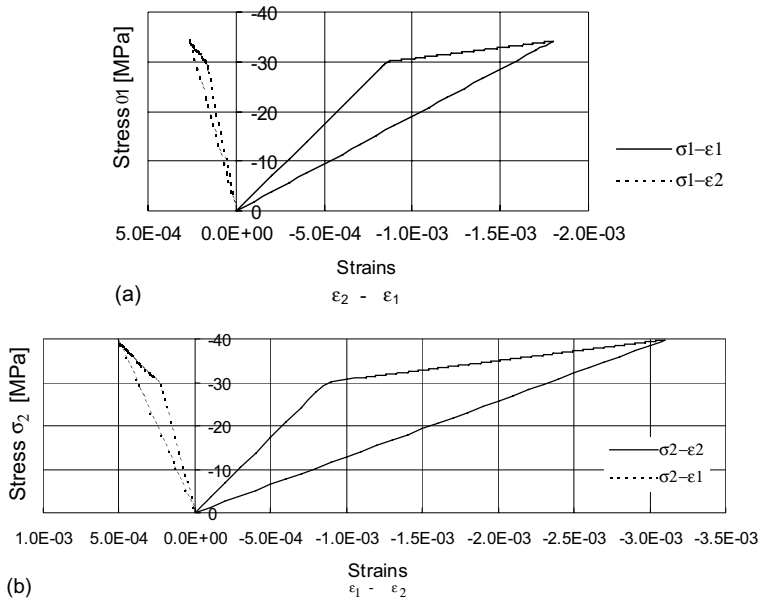

Fig. 12. Stress–strain curves: (a) first load stage and (b) second load stage.

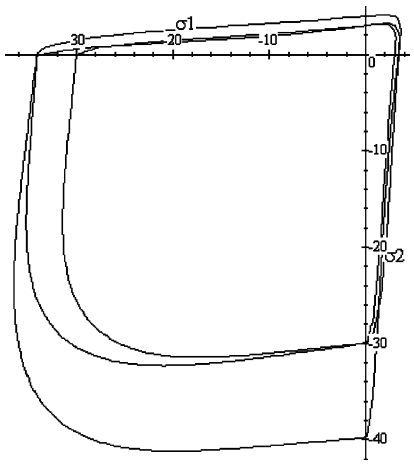

Fig. 13. Initial damage threshold surface (internal) and damage threshold surfaces after the first load stage (intermediate) and after the second load stage (external).

6.2. Numerical test with rotation of principal strain directions

The numerical test proposed by Willam et al. [33] that has been widely used to prove damage and cracking models by other researchers, is the other test presented in this section.

The test consists of two loading stages. In the first step, uniaxial tension is applied in direction x, just until the damage threshold. In the second step, increments of strain components ε_x, ε_y, ε_{xy} are applied in the proportions 1, 1.5, 1 respectively, keeping the out of plane stress components $\sigma_{zz} = \tau_{zx} = \tau_{zy} = 0$. The corresponding strain loading history is shown in Fig. 14. The second loading step represents biaxial extension followed by a rotation of principal strain directions.

The material properties are the following:

Initial elastic modulus:	$E_0 = 10^7$ kPa
Initial Poisson coefficient:	$v = 0.2$
Initial damage threshold in uniaxial compression:	$\sigma_{co} = 10^4$ kPa
Strength damage thresholds ratio:	$n = \sigma_{co}/\sigma_{to} = 1$
Fracture energy:	$G_f = 15$ kPa m
Directional coupling:	$\beta = 0.4$.

The stress–strain response under uniaxial tension, represented by an exponential softening curve, is shown in Fig. 15.

The variations of the stress components and the maximum principal stress obtained for the strain history described with an isotropic scalar damage model [17] and with the directional damage model presented are shown in Figs. 16 and 17 respectively. The difference between the response provided by the scalar damage model and that obtained with the directional damage model is evident. These results confirm the conclusion of Fichant et al. [9] referred to the importance of the induced damage in multiaxial extension problems, like shear-tension problems.

A comparison with the results obtained by Carol et al. [4,5] is shown in Fig. 18. It can be seen that the curves obtained with the directional damage model are similar to those obtained by Carol et al. [4,5]. Sign inversion in tangential stresses and a substantial increase of the stress component in y direction in relation with the results given by the scalar damage model are evident.

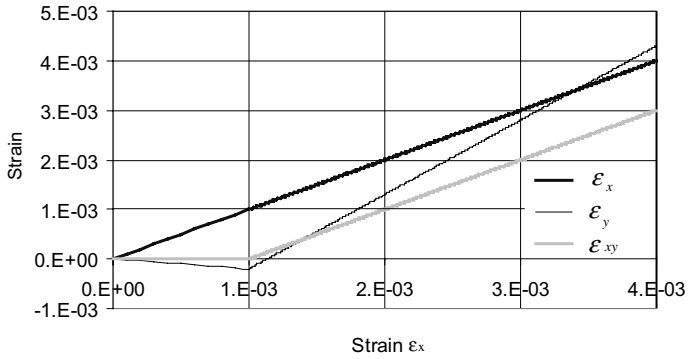

Fig. 14. Load path in the strain space.

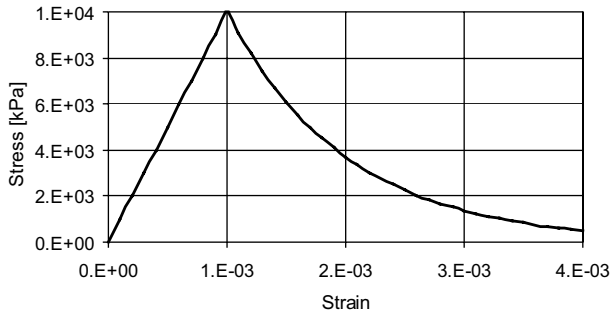

Fig. 15. Uniaxial stress–strain curve.

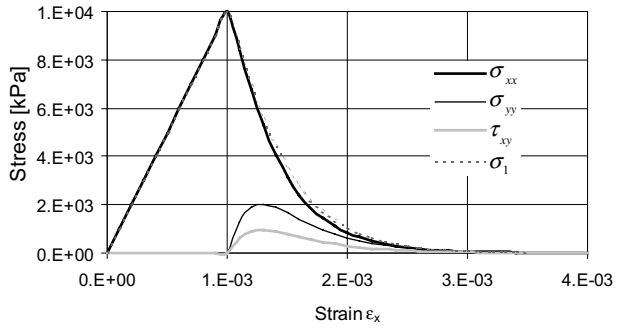

Fig. 16. Evolution of the stress components obtained with a scalar damage model.

The evolutions of the angles between the x-axis and major principal directions of stress, strain and damage obtained with the proposed directional damage model and with a scalar damage model are plotted in Fig. 19. It is clear that, in contrast to the isotropic damage model, due to the directionality of damage, the proposed model leads to principal directions of stress not coincident with the principal directions of strain.

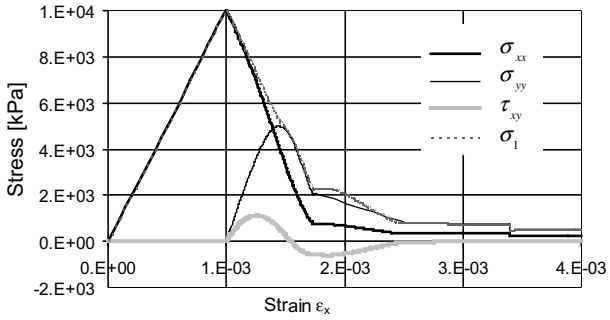

Fig. 17. Evolution of the stress components obtained with the proposed directional damage model.

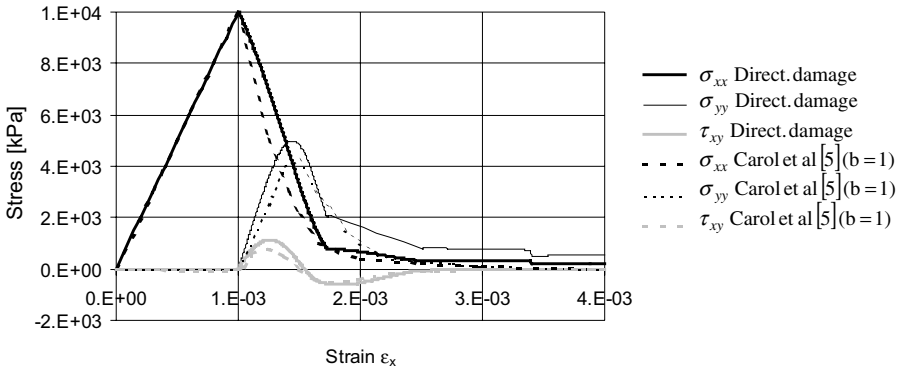

Fig. 18. Comparison with the results obtained by Carol et al. [4,5].

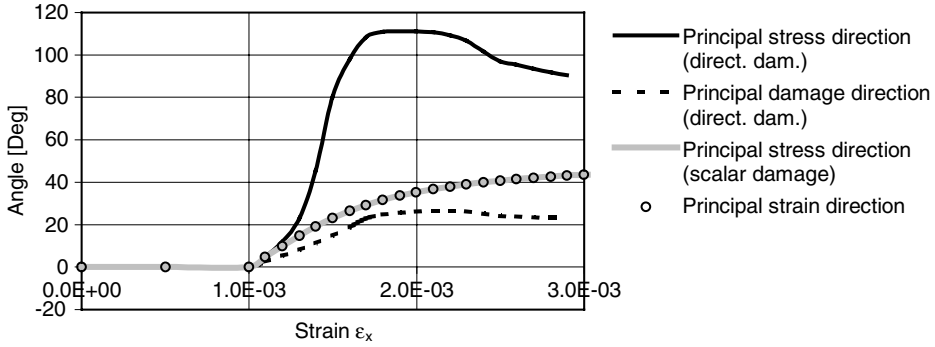

Fig. 19. Evolution of the angles between the x-axis and major principal directions of stress, strain and damage.

Fig. 20 shows the evolution of the components of the second order damage tensor m_{ij} and the comparison with the diagonal value $\sqrt{1-d}$ for the scalar damage model.

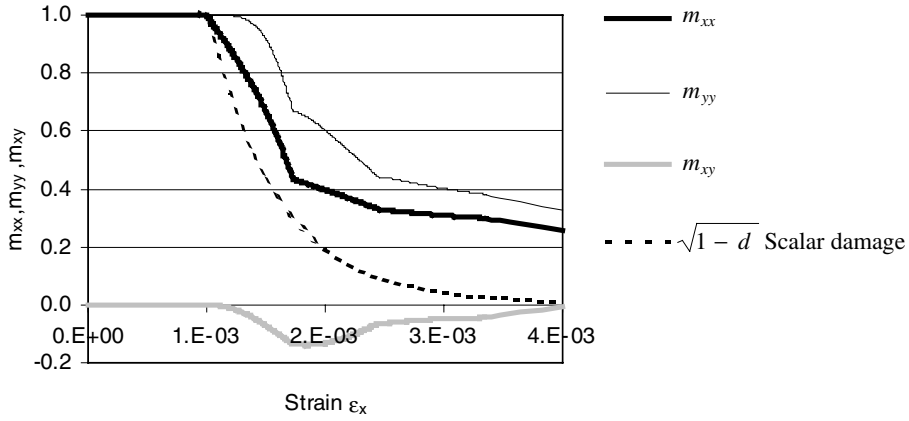

Fig. 20. Evolution of the second order damage tensor components.

6.3. Application example: combined shear and tension in concrete

The tests performed by Van Mier et al. [28] are numerically reproduced in this section. A concrete specimen like that in Fig. 21 was tested under tension, compression shear, tension shear and combined tension and tension shear. Fig. 22 shows the finite element mesh used. The material properties are the following:

Initial elastic modulus:	$E_0 = 30\,000$ Mpa
Initial Poisson coefficient:	$v = 0.2$
Initial damage threshold in uniaxial compression:	$\sigma_{co} = 30$ Mpa
Strength damage thresholds ratio:	$n = \sigma_{co}/\sigma_{to} = 12.1$
Fracture energy:	$G_f = 0.1$ kN/m
Directional coupling:	$\beta = 0.4$
Exponential softening.	

Fig. 23 represents the tension force P versus the relative displacement δ for the tension test. The curves corresponding to experimental results [28] and those obtained with an isotropic damage model [17] and

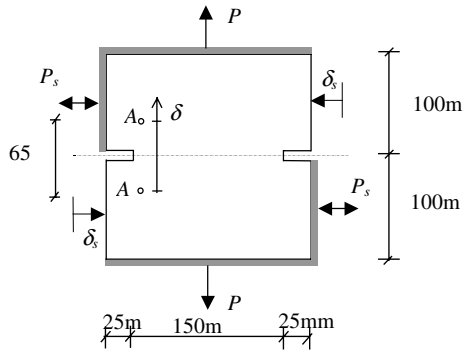

Fig. 21. Specimens tested by Van Maier et al. [28].

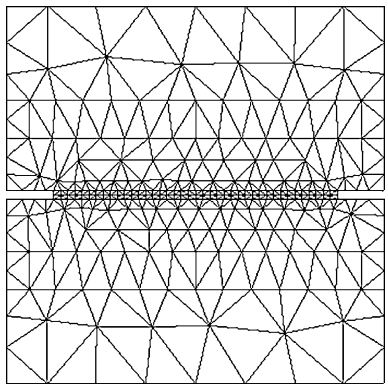

Fig. 22. Finite element mesh.

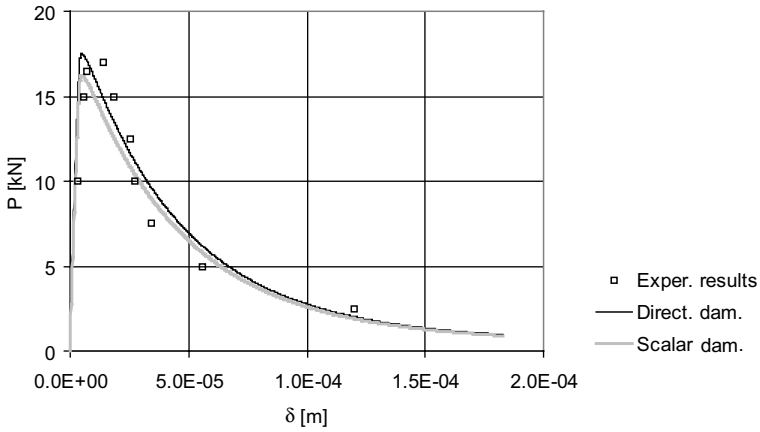

Fig. 23. Tension test.

with the proposed anisotropic damage model are presented. From Fig. 23 it is clear that numerical results obtained with both models are similar to experimental results.

The results corresponding to compression shear and tension shear tests are presented in Fig. 24. There are no experimental results for the tension shear tests and the experimental results for the compression shear test do not reach the failure load. As in the case of tension, the results obtained with the scalar damage model and with the directional damage model are similar and follow experimental ones.

Finally, the influence of previous cracking on shear resistance is studied. The specimen was first subjected to tension in displacement control. After loading it to a prescribed axial cracking opening, the specimen was unloaded to $P = 0$. Subsequently tension shear was applied while maintaining $P = 0$. This allowed for an unrestrained opening of the crack during shear.

Fig. 25 shows the shear strength as a function of the previous crack opening obtained in the experimental tests and with both damage models. It is clear that the scalar damage model leads to an abrupt drop in the shear strength, proportional to the drop in tensile strength, while the directional damage model accurately reproduces experimental results for the shear strength.

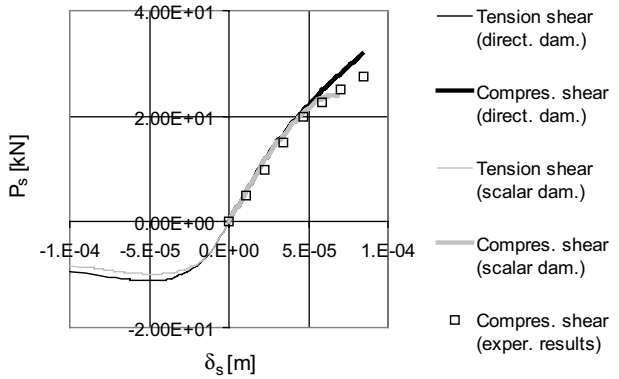

Fig. 24. Tension shear and compression shear tests.

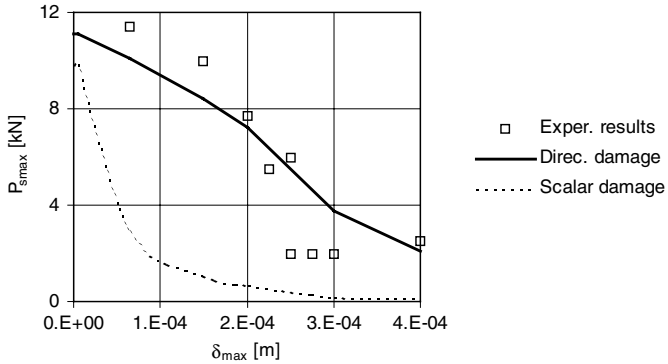

Fig. 25. Effect of previous cracking on tension shear strength.

7. Conclusions

A 'directional damage model' based on the assumption of existence of a 'fictitious non-damaged space' whose variables are related to the variables in the 'real damage space' through kinematics transformation is presented in this paper. This fact allows the use of a finite element computer program originally developed for simulating the finite strains and makes it straightforward the extension to the case of anisotropic damage in finite strain problems.

The space transformation definition is based on the physical interpretation of damage of reduction in effective area, extended to the directional damage case. This physical interpretation of damage allows defining directional damage by a symmetric 'second order damage tensor' and gives directly, a symmetric secant stiffness tensor. The damage tensor results similar to the symmetrizations proposed by other authors [4,5,30].

The basic equations of the model that define the damage threshold and its evolution have been derived from the thermodynamics of irreversible processes theory.

A simple return-mapping algorithm for the numerical integration of the resulting constitutive equations has been developed.

The application examples presented show the capacity of the model to predict directional damage not only in proportional loading cases but also in problems where rotation of principal strains directions are

involved. The results obtained are similar to those obtained by other authors with models based on different assumptions [4,5].

Acknowledgements

The financial support of CONICET and National University of Tucumán is gratefully acknowledged.

Appendix A. Summary of the model

A summary of the model equations necessary for its numerical implementation is presented in this section.

Secant equation:

$$\sigma_{ij} = \frac{\partial \Psi}{\partial \varepsilon_{ij}} = C_{ijrs}\varepsilon_{rs}, \quad C_{ijkl} = M_{ijmn}\overline{C}_{mnpq}M_{pqkl}, \quad M_{ijmn} = m_{ik}m^{t}_{jn}.$$

Damage threshold function:

$$F = \sqrt{\frac{1}{2}\tilde{y}_{ij}\tilde{y}_{ij}} - 1 = 0, \quad \tilde{y}_{ij} = \widetilde{A}_{ijkl}\bar{y}_{kl} = A_{ijkl}\overline{A}_{klpq}y^{m}_{pq},$$

$$\widetilde{A}_{ijkl} = B_{ik}C_{jl}, \quad B_{ik} = \frac{E_o}{\sqrt{2}}\delta_{is}\delta_{ks}m^{5}_{s}, \quad C_{ij} = \delta_{ir}\delta_{jr}\{\sigma[(1-\beta)m_r + \beta \det m_{kl}]\}^{-2},$$

$$\overline{A}_{ijkl} = (n^2-1)\delta_{im}\delta_{jm}\delta_{km}\delta_{lm}r_m + \delta_{im}\delta_{jn}\delta_{km}\delta_{ln}\delta_{mn}, \quad r_m = \frac{\langle \sigma_m \rangle}{|\sigma_m|}, \quad \text{no sum over } m,$$

$$y^{m}_{ij} = -\frac{\partial \Psi}{\partial m_{ij}} = -\frac{1}{2}\varepsilon_{kl}\frac{\partial C_{klpq}}{\partial m_{ij}}\varepsilon_{pq}.$$

Damage potential function:

$$G = \sqrt{\frac{1}{2}\tilde{y}_{ij}\tilde{y}_{ij}} - 1 = 0.$$

Damage flow rule:

$$\dot{m}_{ij} = \dot{\lambda}\frac{\partial G(Y)}{\partial y^{m}_{ij}} = \dot{\lambda}\frac{\partial G(Y)}{\partial \tilde{y}_{pq}}\frac{\partial \tilde{y}_{pq}}{\partial \bar{y}_{kl}}\frac{\partial \bar{y}_{kl}}{\partial y^{m}_{ij}} \approx \dot{\lambda}\frac{\tilde{y}_{pq}}{\sqrt{\frac{1}{2}\tilde{y}_{rs}\tilde{y}_{rs}}}\widetilde{A}_{pqkl}\overline{A}_{klij}.$$

Damage consistency condition:

$$\dot{F} = 0 \Rightarrow \frac{\partial F}{\partial \varepsilon_{kl}}\dot{\varepsilon}_{kl} + \frac{\partial F}{\partial m_{ij}}\dot{m}_{ij} = 0,$$

$$\frac{\partial F}{\partial y^{m}_{ij}}\frac{\partial y^{m}_{ij}}{\partial \varepsilon_{kl}}\dot{\varepsilon}_{kl} + \frac{\partial F}{\partial m_{kl}}\dot{\lambda}\frac{\partial G}{\partial y^{m}_{kl}} = 0 \Rightarrow \dot{\lambda} = -\frac{\dfrac{\partial F}{\partial y^{m}_{ij}}\dfrac{\partial y^{m}_{ij}}{\partial \varepsilon_{kl}}\dot{\varepsilon}_{kl}}{\dfrac{\partial F}{\partial m_{kl}}\dfrac{\partial G}{\partial y^{m}_{kl}}},$$

where

$$\frac{\partial F(Y)}{\partial y_{ij}^m} = \frac{\partial F(Y)}{\partial \tilde{y}_{pq}} \frac{\partial \tilde{y}_{pq}}{\partial \bar{y}_{kl}} \frac{\partial \bar{y}_{kl}}{\partial y_{ij}^m} = \frac{\partial F(Y)}{\partial \tilde{y}_{pq}} \widetilde{A}_{pqkl} \overline{A}_{klij},$$

$$\frac{\partial F(Y)}{\partial \tilde{y}_{pq}} = \frac{\tilde{y}_{pq}}{\sqrt{\frac{1}{2}\tilde{y}_{rs}\tilde{y}_{rs}}},$$

$$\begin{aligned}\frac{\partial y_{ij}^m}{\partial \varepsilon_{kl}} = &-\frac{1}{2}\left[\delta_{ik} m_{ls}^t \overline{C}_{jsmn} m_{mp} m_{nq}^t \varepsilon_{pq} + \varepsilon_{ir} m_{rs}^t \overline{C}_{jsmn} m_{mk} m_{nl}^t\right] - \frac{1}{2}\left[\delta_{jl} m_{ks} \overline{C}_{simn} m_{mp} m_{nq}^t \varepsilon_{pq} + \varepsilon_{rj} m_{rs} \overline{C}_{simn} m_{mk} m_{nl}^t\right] \\ &-\frac{1}{2}\left[m_{kp} m_{lq}^t \overline{C}_{pqim} m_{mn}^t \varepsilon_{jn} + \varepsilon_{rs} m_{rp} m_{sq}^t \overline{C}_{pqim} m_{ml}^t \delta_{jk}\right] - \frac{1}{2}\left[m_{kp} m_{lq}^t \overline{C}_{pqmj} m_{mn} \varepsilon_{ni} + \varepsilon_{rs} m_{rp} m_{sq}^t \overline{C}_{pqmj} m_{mk} \delta_{il}\right],\end{aligned}$$

$$\frac{\partial F(Y)}{\partial m_{ij}} = \frac{\partial F(Y)}{\partial \tilde{y}_{pq}} \frac{\partial \tilde{y}_{pq}}{\partial m_{ij}} = \frac{\partial F(Y)}{\partial \tilde{y}_{pq}} \left[\frac{\partial (\widetilde{A}_{pqkl} \overline{A}_{klrs})}{\partial m_{ij}} y_{rs}^m + \widetilde{A}_{pqkl} \overline{A}_{klrs} \frac{\partial y_{rs}^m}{\partial m_{ij}}\right],$$

$$\begin{aligned}\frac{\partial y_{ij}^m}{\partial m_{kl}} = &-\frac{1}{2}\left[\varepsilon_{il} \overline{C}_{jkmn} m_{mp} m_{nq}^t \varepsilon_{pq} + \varepsilon_{im} m_{mp}^t \overline{C}_{jpkn} m_{nq}^t \varepsilon_{lq} + \varepsilon_{in} m_{nq}^t \overline{C}_{jqml} m_{mp} \varepsilon_{pk}\right] \\ &-\frac{1}{2}\left[\varepsilon_{kj} \overline{C}_{limn} m_{mp} m_{nq}^t \varepsilon_{pq} + \varepsilon_{mj} m_{mp} \overline{C}_{pikn} m_{nq}^t \varepsilon_{lq} + \varepsilon_{nj} m_{nq} \overline{C}_{qiml} m_{mp} \varepsilon_{pk}\right] \\ &-\frac{1}{2}\left[\varepsilon_{kp} m_{pq}^t \overline{C}_{lqim} m_{mn}^t \varepsilon_{jn} + \varepsilon_{ql} m_{qp} \overline{C}_{pkim} m_{mn}^t \varepsilon_{jn} + \varepsilon_{mn} m_{mp} m_{nq}^t \overline{C}_{pqil} \varepsilon_{jk}\right] \\ &-\frac{1}{2}\left[\varepsilon_{kp} m_{pq}^t \overline{C}_{lqmj} m_{mn} \varepsilon_{ni} + \varepsilon_{ql} m_{qp} \overline{C}_{pkmj} m_{mn} \varepsilon_{ni} + \varepsilon_{mn} m_{mp} m_{nq}^t \overline{C}_{pqkj} \varepsilon_{li}\right].\end{aligned}$$

Primary field energy dissipation:

$$\Xi_m = Y_i \dot{\chi}_i = y_{ij}^m \dot{m}_{ij} = \dot{\lambda} y_{ij}^m \frac{\partial G}{\partial y_{ij}^m} \geqslant 0 \quad \text{Because } \dot{\lambda} \geqslant 0 \text{ and } G(y_{ij}^m) \text{ is convex.}$$

Tangent stiffness:

$$\dot{\sigma}_{ij} = \dot{C}_{ijrs} \varepsilon_{rs} + C_{ijrs} \dot{\varepsilon}_{rs},$$

$$\begin{aligned}\dot{C}_{ijrs} &= \dot{M}_{ijmn} \overline{C}_{mnpq} M_{pqrs} + M_{ijmn} \overline{C}_{mnpq} \dot{M}_{pqrs} \\ &= \dot{m}_{im} m_{jn}^t \overline{C}_{mnpq} m_{pr} m_{qs}^t + m_{im} \dot{m}_{jn}^t \overline{C}_{mnpq} m_{pr} m_{qs}^t + m_{im} m_{jn}^t \overline{C}_{mnpq} \dot{m}_{pr} m_{qs}^t + m_{im} m_{jn}^t \overline{C}_{mnpq} m_{pr} \dot{m}_{qs}^t \\ &= \dot{\lambda}\left(\frac{\partial G}{\partial y_{im}^m} m_{jn}^t \overline{C}_{mnpq} m_{pr} m_{qs}^t + m_{im} \frac{\partial G}{\partial y_{nj}^m} \overline{C}_{mnpq} m_{pr} m_{qs}^t\right) \\ &\quad + \dot{\lambda}\left(m_{im} m_{jn}^t \overline{C}_{mnpq} \frac{\partial G}{\partial y_{pr}^m} m_{qs}^t + m_{im} m_{jn}^t \overline{C}_{mnpq} m_{pr} \frac{\partial G}{\partial y_{sq}^m}\right),\end{aligned}$$

$$\dot{\sigma}_{ij} = C_{ijrs}\dot{\varepsilon}_{rs} - \frac{\dfrac{\partial F}{\partial y^m_{tu}}\dfrac{\partial y^m_{tu}}{\partial \varepsilon_{rs}}\dot{\varepsilon}_{rs}}{\dfrac{\partial F}{\partial m_{tu}}\dfrac{\partial G}{\partial y^m_{tu}}}\left(\frac{\partial G}{\partial y^m_{im}} m^t_{jn}\overline{C}_{mnpq} m_{pk} m^t_{ql} + m_{im}\frac{\partial G}{\partial y^m_{nj}}\overline{C}_{mnpq} m_{pk} m^t_{ql} + m_{im} m^t_{jn}\overline{C}_{mnpq}\frac{\partial G}{\partial y^m_{pk}} m^t_{ql}\right.$$

$$\left. + m_{ik} m^t_{jn}\overline{C}_{mnpq} m_{pk}\frac{\partial G}{\partial y^m_{lq}}\right)\varepsilon_{kl}$$

$$= C^T_{ijrs}\dot{\varepsilon}_{rs},$$

$$C^T_{ijrs} = C_{ijrs} - \frac{\left[\left(\dfrac{\partial G}{\partial y^m_{im}} m^t_{jn} + m_{im}\dfrac{\partial G}{\partial y^m_{nj}}\right)\bar{\sigma}_{mn} + m_{im} m^t_{jn}\overline{C}_{mnpq}\left(\dfrac{\partial G}{\partial y^m_{pk}} m^t_{ql} + m_{pk}\dfrac{\partial G}{\partial y^m_{lq}}\right)\varepsilon_{kl}\right]\dfrac{\partial F}{\partial y^m_{tu}}\dfrac{\partial y^m_{tu}}{\partial \varepsilon_{rs}}}{\dfrac{\partial F}{\partial m_{tu}}\dfrac{\partial G}{\partial y_{tu}}}.$$

References

[1] M. Ashby, B. Tomkins, in: Smith, Miller (Eds.), Proceedings, ICM-3, Oxford Pergamon, 1980.
[2] A.G. Atkins, Y.W. Mai, Elastic and Plastic Fracture, Metals, Polymers, Ceramics, Composite, Biological Materials, Ellis Horwood, 1988.
[3] I. Carol, E. Rizzi, K. Willam, A unified description of elastic degradation and damage based on loading surface, Int. J. Solids Struct. 31 (1994) 2835–2865.
[4] I. Carol, E. Rizzi, K. Willam, On the formulation of anisotropic degradation using a pseudo-logarithmic damage tensor, Structural Engineering and Structural Mechanics Research Series Report CU/SR-98/1, University of Colorado at Boulder, 1998.
[5] I. Carol, E. Rizzi, K. Willam, On the formulation of anisotropic degradation II. Generalized pseudo Rankine model for tensile damage, Int. J. Solids Struct. 38 (2001) 519–543.
[6] J.P. Cordebois, F. Sidoroff, Damage-induced elastic anisotrophy, in: J.P. Boehler (Ed.), Mechanical Behavior of Anisotropic Solids, Colloque Euromech 115, Villard de Lans, Martinus Nijhoff, Dordrecht, The Netherlands, 1979, pp. 761–774.
[7] J.L. Chaboche, Continuum damage mechanics, anisotropy and damage deactivation for brittle materials like concrete and ceramic composites, Int. J. Damage Mech. 4 (1995) 5–22.
[8] A. Dragon, Z. Mroz, A continuum damage model for plastic–brittle behaviour of concrete, Int. J. Engrg. Sci. 17 (1979) 121–137.
[9] S. Fichant, C. La Borderie, G. Pijaudier-Cabot, Isotropic and anisotropic descriptions of damage in concrete structures, Mech. Cohesive-Frictional Mater. 4 (1999) 339–359.
[10] J.W. Ju, On energy-based coupled elastoplastic damage theories: constitutive modeling and computational aspects, Int. J. Solids Struct. 25 (7) (1989) 803–833.
[11] J.W. Ju, Isotropic and anisotropic damage variables in continuum damage mechanics, ASCE J. Engrg. Mech. 16 (12) (1990) 2764–2770.
[12] L.M. Kachanov, Time of the rupture process under creep conditions, IVZ Akad. Nauk. SSR (Otd Tech Nauk) 8 (1958).
[13] D. Krajcinovic, G.U. Fonseka, The continuous damage theory of brittle materials, Part I and II, J. Appl. Mech., ASME 48 (1981) 809–824.
[14] D. Krajcinovic, Continuous damage mechanics revisited: basic concepts and definitions, J. Appl. Mech. 52 (1985) 829–834.
[15] J. Lemaitre, J.L. Chaboche, Aspecta Phenoménologique de la Rupture par Endommagement, J. Mec. Théorique Apl. (1978) 317–365.
[16] J. Lemaitre, R. Desmorat, M. Sauzy, Anisotropic damage law of evolution, Eur. J. Mech. A/Solids 19 (2000) 187–208.
[17] B. Luccioni, S. Oller, R. Danesi, Coupled plastic-damaged model, Comput. Meth. Appl. Mech. Engrg. 129 (1996) 81–89.
[18] J. Lubliner, On the thermodynamic foundations of non-linear mechanics, Int. J. Non-Lin. Mech. 7 (1972) 237–254.
[19] L. Malvern, Introduction to the Mechanics of Continuos Medium, Prentice Hall, USA, 1969.
[20] G.A. Maugin, The Thermomechanics of Plasticity and Fracture, Cambridge University, 1992.
[21] J. Mazars, G. Pijaudier-Cabot, Continuum damage theory—application to concrete, J. Engrg. Mech. ASCE 115 (1989) 345–365.
[22] J. Moreau, Functionelles Convexes, Polycopié Collége de France, Paris, 1966.

[23] S. Murakami, N. Ohno, A continuum theory of creep and creep damage, in: 3rd IUTAM Symposium on Creep in Structure, Leicester, 1980.
[24] M. Ortiz, A constitutive theory for the inelastic behaviour of concrete, Mech. Mater. 4 (1985) 67–93.
[25] F. Sidoroff, Description of anisotropic application to elasticity, in: J. Hult, J. Lemaitre (Eds.), Physical Non-Linearities in Structural Analysis, IUTAM Series, Springer, New York, 1980, pp. 237–244.
[26] C. Simo, J. Ju, Stress and strain based continuum damage models. Part I and II, Int. J. Solids Struct. 23 (1987) 375–400.
[27] K.C. Valanis, A global damage theory and the hyperbolicity of the wave problem, J. Appl. Mech. ASME 58 (1991) 311–316.
[28] J.G.M. Van Mier, N.B. Nooru-Mohamed, G. Timmers, An experimental study of shear fracture and aggregate interlock in cement based composites, Heron 36 (4) (1991).
[29] G.Z. Voyiadjis, P.I. Kattan, A plasticity-damage theory for large deformation of solids-I. Theoretical formulation, Int. J. Engrg. Sci. 30 (9) (1992) 1089–1108.
[30] G.Z. Voyiadjis, T. Park, Anisotropic damage effect tensors for the symmetrization of the effective stress tensor, Trans. ASME 64 (1997) 106–110.
[31] G.Z. Voyiadjis, T. Park, Kinematics of large elastoplastic damage deformation, in: G.Z. Voyiadjis, J.W.W. Ju, J.L. Chaboche (Eds.), Damage Mechanics in Engineering Materials, Elsevier Science, 1998, pp. 45–63.
[32] G.Z. Voyiadjis, B. Deliktas, A coupled anisotropic damage model for the inelastic response of composite materials, Comput. Meth. Appl. Mech. Engrg. 183 (2000) 159–199.
[33] K. Willam, E. Pramono, S. Sture, Fundamental issues of smeared crack models, in: S.P. Shah, S.E. Swartz (Eds.), SEM-RILEM Int. Conf. on Fracture of Concrete and Rock, Society of Engineering Mechanics, Bethel, CT, 1987, pp. 192–207.
[34] Q. Yang, W.Y. Zhou, G. Sowoboda, Micromechanical identification of anisotropic evolution laws, Int. J. Fract. 98 (1999) 55–76.
[35] O.C. Zienkiewicz, R. Taylor, El Método los Elementos Finitos, vol. 1, McGraw Hill, CIMNE, 1994.